

RESEARCH PAPER



SIX1 and *DACH1* influence the proliferation and apoptosis of hepatocellular carcinoma through regulating p53

Qi Cheng^a, Deng Ning^b, Jin Chen^a, Xue Li^c, Xiao-Ping Chen^a, and Li Jiang^b

^aHepatic Surgery Center, Tongji Hospital, Tongji Medical College, Huazhong University of Science and Technology, Wuhan, Hubei, China; ^bDepartment of Biliary and Pancreatic Surgery, Tongji Hospital, Tongji Medical College, Huazhong University of Science and Technology, Wuhan, Hubei, China; ^cDepartment of Clinical Immunology, School of Laboratory Medicine, Tianjin Medical University, Tianjin, China

ABSTRACTS

This research aimed to explore effects of *SIX1* and *DACH1* on hepatocellular carcinoma (HCC) cell proliferation, apoptosis and cell cycle. Fifty paired hepatocellular carcinoma tissues were screened for differentially expressed genes. *SIX1* and *DACH1* expressions were subjected to qRT-PCR and western blot in tumor tissues and cells. The knockdown efficiency of siRNAs and transfection efficiency of cDNAs and siRNAs were validated by qRT-PCR and western blot as well. Then colony formation assay and flow cytometry were applied to observe cell proliferation, cell apoptosis and cell cycle changes. Immunofluorescence co-localization and immunoprecipitation were used to analyze the interaction between proteins which was quantified using western blot. Effects of *SIX1* and *DACH1* on tumor growth and their expressions in tumors were confirmed *in vitro* in nude mice model. Results of these experiments showed that *SIX1* was overexpressed while *DACH1* was suppressed in HCC tissues and cells. The suppression of *SIX1* and overexpression of *DACH1* not only inhibited cell proliferation, but also induced cell apoptosis and arrested cell cycle in G2/M phase compared with control group. Results of immunofluorescence co-localization suggested that *SIX1*, p53 and *DACH1* were significantly overlapped. Immunoprecipitation showed that *DACH1* (marked with Flag tag) could pull down p53 and *SIX1*, but *SIX1* (marked with His tag) could only pull down *DACH1*, which indicated that an indirect regulation between *SIX1* and p53. Validated with western blot afterwards, *DACH1* overexpression suppressed tumorigenesis *in vivo* by up-regulating p53 expression while *SIX1* overexpression accelerated tumor growth by down-regulating p53 expression. Therefore, the decrease of *SIX1* facilitated the expression of *DACH1*, thus activated the expression of p53 and suppressed the progression of HCC both *in vitro* and *in vivo*.

ARTICLE HISTORY

Received 16 October 2017
Revised 19 December 2017
Accepted 29 December 2017

KEYWORDS

apoptosis; *DACH1*;
hepatocellular carcinoma;
SIX1; p53; proliferation

Introduction

Hepatocellular carcinoma (HCC) is the fourth most commonly diagnosed cancer and the second primary cause of cancer-related death.¹ Numerous advances have been achieved in the understanding of the molecular basis of HCC. However, the molecular mechanisms that define the relationships between early environmental cues and disease phenotypes are poorly understood. Main reasons are that these interactions are complex, difficult to quantify accurately, and often occur over long periods of time.²

SIX1, a member of the SIX families of homeodomain transcription factors, is essential for the development of numerous organs.³ In fact, it is considered as an oncofetal protein because dysregulation and inappropriate re-expression of *SIX1* can result in genomic instability, malignant transformation, and metastasis in animal models and humans.² Overexpression of *SIX1* has been found in various human cancers and is associated with increased tumor progression, metastasis, and decreased survival.³ *SIX1* can promote colorectal cancer growth and metastasis through increasing features of cancer stem cells, and stimulate angiogenesis by up-regulating vascular endothelial growth factor (VEGF).³

Additionally, increased *SIX1* level is associated with poor survival outcome of osteosarcoma patients.⁴ However, the biological function of *SIX1* in HCC is rarely investigated.

Dachshund homolog 1 (*DACH1*), a fundamental component of the Retinal Determination Gene Network, is frequently expressed in epithelial cells. *DACH1* abundance is decreased in a variety of malignancies, involving organs including breast, prostate, liver, lung, and brain. Massive evidence suggested that *DACH1* might function as a new type of tumor suppressor.⁵ Ke Chen et al identified *DACH1* as a novel p53 binding partner that participated in p53-mediated induction of p21 and cell cycle arrest.⁶ The knockdown of *DACH1* arrested the cell cycle progression in myeloid progenitor cells,⁷ which also suggested its regulation on cell cycle changes in HCC.

Studies have found that *DACH1* was correlated with the expression of *SIX1*.^{8,9} For instance, Miller et al. identified the protein-protein interaction of SIX and DACH in malignant peripheral nerve sheath tumors.¹⁰ P53 is another important molecule in tumor apoptosis and can bind to *DACH1* which therefore blocks the propagation in lung adenocarcinoma cells.^{11,6} In spite of

current researches, discussions of the relationship between *SIX1* and p53 remain in shortage.

MDM2 interacts with p53 is common in HCC. *MDM2* binds p53 at its transactivation domain and blocks p53-mediated transcriptional regulation, and p53 regulates *MDM2* transcription through p53-specific response elements in the promoter region of *MDM2*, thus forming an auto-regulatory feedback loop.^{12,13} Therefore, *MDM2* expression together with p53 expression was evaluated in this study.

Here we evaluated *SIX1* and *DACH1* expressions in HCC and their functional mechanism on tumor growth. The possible mechanism behind the regulation was explored by monitoring p53 protein expressions. These findings may provide new references for the study on the molecular mechanism of hepatocellular carcinoma, contributing to the therapeutic strategy and the reduction of mortality rates of HCC in the future.

Results

High expression of *SIX1* and low expression of *DACH1* in HCC were detected

To screen out aberrantly expressed genes, we examined 50 cases of hepatocellular carcinoma tissue samples and 50 adjacent tissue samples. Among all differentially expressed genes, five high expressed genes and five low expressed genes respectively were selected to draw the heat map. *SIX1* was high expressed in hepatocellular carcinoma tissues and *DACH1* was low expressed in hepatocellular carcinoma tissues (Fig. 1A). Both genes showed significant statistical significance ($P < 0.05$) (Fig. 1B). Log fold-change value and P value of *SIX1* and *DACH1* expressions were shown in Table 2. A positive log fold-change value of *SIX1* indicated a higher expression in tumor tissues compared with adjacent ones. A negative log fold-change value of *DACH1* indicated a lower expression in tumor tissues compared with adjacent ones. In order to further validate the results of microarray analysis, we carried out RT-qPCR on 50 pairs of samples. RT-qPCR results also showed that *SIX1* was high expressed and *DACH1* was low expressed in hepatocellular carcinoma tissues (both $P < 0.001$, Fig. 1C–D). Five pairs of patient samples were randomly selected, and protein expression differences between *SIX1* and *DACH1* was detected by Western Blot, confirming the high expression of *SIX1* protein and the low expression of *DACH1* protein (Fig. 1E). These results suggested that *SIX1* and *DACH1* may be potential predictors of HCC. In order to study the effects of *SIX1* and *DACH1* on the function of HCC cells, we examined the expression of *SIX1* and *DACH1* in three HCC cell lines (SK-HEP-1, Huh-7 and HepG2) and normal cell line HL-7702[L-02] (Fig. 1F). Compared with normal HCC cell line HL-7702 [L-02], *SIX1* was high expressed in HCC while *DACH1* was low expressed in HCC. HepG2 cells displayed generally the most significant changes and therefore were selected for further functional experiment study.

SIX1 promoted but *DACH1* inhibited HCC progression

Three siRNAs for *SIX1* and *DACH1* respectively were pre-tested for the choice of most suitable siRNA to knock down the expression of *SIX1* and *DACH1*. According to protein expressions shown in Fig. 2A–B, si-*SIX1*-2, si-*SIX1*-3 and si-*DACH1*-1, si-

DACH1-3 presented better knockdown efficiency and therefore were chosen for following experiments. Overexpression (cDNA) and downregulation (siRNAs) of *SIX1* and *DACH1* (Fig. 2C–F) were confirmed by qPCR and western blot. cDNA-*SIX1* greatly up-regulated *SIX1* expression and si-*SIX1* markedly down-regulated *SIX1* mRNA and protein expressions. Similarly, cDNA-*DACH1* significantly enhanced *DACH1* expression while si-*DACH1* drastically suppressed *DACH1* mRNA expression and protein expression (Fig. 2C–D). Following the validation of transfection efficiency, colony formation assay further tested influences of *SIX1* and *DACH1* on the cell proliferation ability. Results indicated that *SIX1* overexpression increased colony numbers and *SIX1* knockdown decreased colony numbers. On the contrary, high expression of *DACH1* inhibited colony formation and low expression of *DACH1* promoted colony formation (Fig. 2E–F) ($P < 0.05$). These results suggested that *SIX1* could promote whereas *DACH1* could inhibit HCC proliferation. Besides, si-*SIX1*-2 and si-*SIX1*-3 could efficiently suppress the proliferation and si-*DACH1*-1 and si-*DACH1*-3 could reversely improve the proliferation (Fig. 3A–B). Flow cytometry results further evaluated influences of *SIX1* and *DACH1* on cell apoptosis as well as on cell cycle. Cell apoptosis assay showed that overexpression of *SIX1* reduced cell apoptosis rate but overexpression of *DACH1* increased cell apoptosis rate ($P < 0.05$), this suggested that *SIX1* acted as an inhibitor while *DACH1* played a role of promoter in cell apoptosis. The inhibition of *SIX1* and *DACH1* validated the above results. The knockdown of *SIX1* could promote cell apoptosis rate while the inhibition of *DACH1* expression efficiently restrained cell apoptosis progress (Fig. 3C–D). Cell cycle assay showed that cells were retarded at G2 / M phase when *SIX1* was inhibited and when *DACH1* was overexpressed. Besides, cells arrested in G2/M phase were reduced in cDNA-*SIX1* group and si-*DACH1*-1 and si-*DACH1*-3 group (Fig. 4A–B, $P < 0.05$). Cell cycle related proteins were tested as well to further confirm cell cycle changes. P21 expression was increased and CDK1 expression was decreased when *SIX1* was inhibited in si-*SIX1*-2 and si-*SIX1*-3 group. However, p21 expression was inhibited and CDK1 expression was elevated in cDNA-*SIX1* group. Similarly, p21 expression was suppressed and CDK1 expression was elevated in si-*DACH1*-1 group and si-*DACH1*-3 group while p21 was increased and CDK1 expression was decreased in cDNA-*DACH1* group (Fig. 4C–D).

SIX1/DACH1 regulated p53 expression

Immunofluorescence co-localization experiments ensured that antibodies bound to the correct target proteins. For instance, perfect co-localization was observed for proteins *DACH1* and p53 whereas co-localization of *SIX1* revealed that *SIX1* could bind to *DACH1* as well (Fig. 5A–B). Co-immunoprecipitation was used to analyze protein-protein interactions. The results showed that *DACH1* labeled by Flag tag co-precipitated p53 and *SIX1*, while *SIX1* marked by HIS tag co-precipitated *DACH1* protein. These results indicated that *DACH1* interacted with *SIX1* and p53 while *SIX1* could only interact with *DACH1* (Fig. 5C). Interactions among *DACH1*, *SIX1*, p53 and *MDM2* were further validated with western blot. *DACH1* and p53 protein expressions were inversely correlated with the expression of *SIX1* ($P < 0.05$). *SIX1* overexpression suppressed expressions

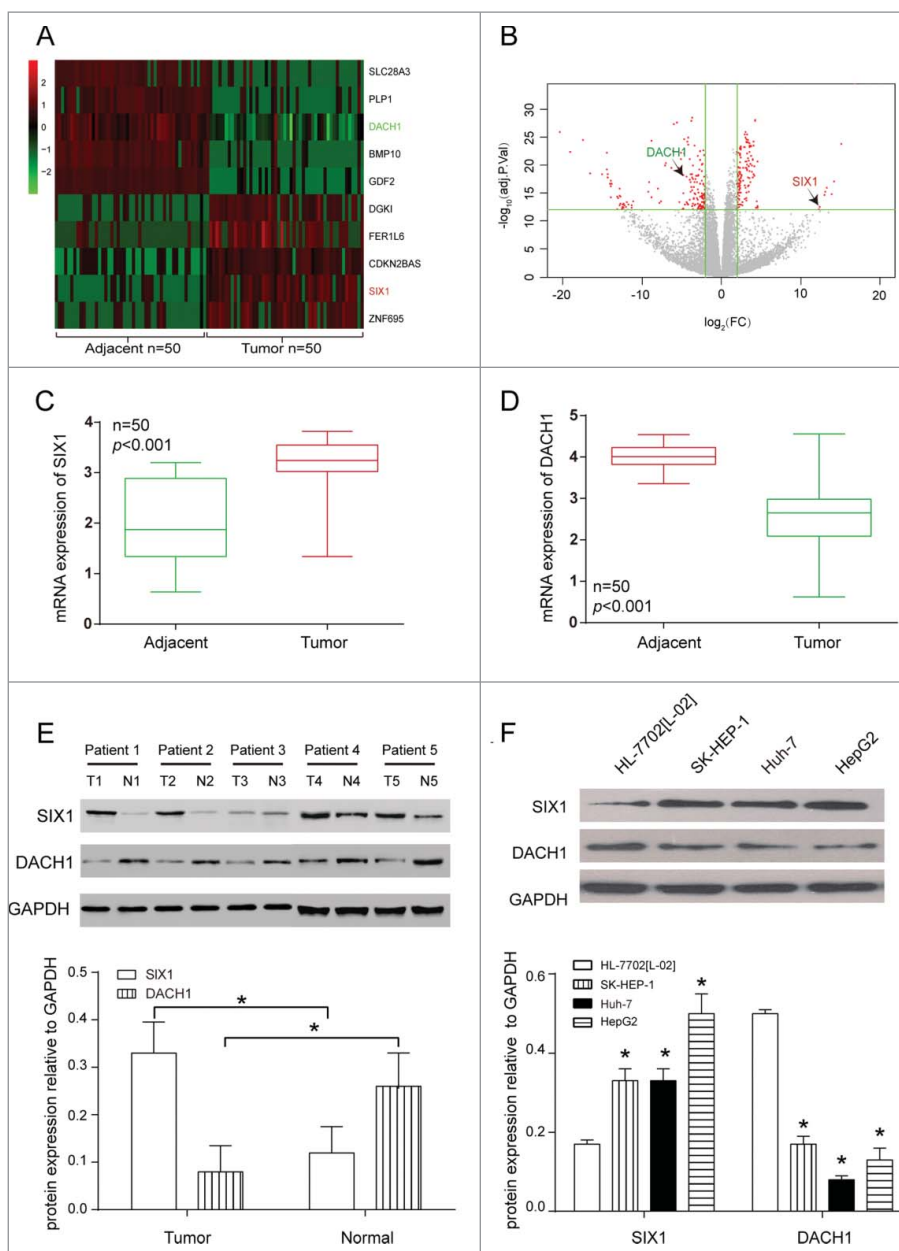


Figure 1. *SIX1* was high expressed and *DACH1* was low expressed in HCC tissues and cells. (A) Heat map showed that *SIX1* was high expressed and *DACH1* was low expressed in HCC tissues compared with adjacent tissues. (B) Volcano plot of *SIX1* overexpression and *DACH1* suppression showed statistical significance ($P < 0.05$). (C-D) RT-qPCR analysis showed high expression of *SIX1* mRNA and low expression of *DACH1* mRNA in 50 samples ($P < 0.001$). (E) WB results showed the high expression of *SIX1* and the low expression of *DACH1* in HCC tissues of five patients. (F) *SIX1* was high expressed and *DACH1* was low expressed in three kinds of HCC cell lines (SK-HEP-1, Huh-7 and HepG2) compared with normal human hepatoma cell line (HL-7702 [L-02]).

of *DACH1* and p53. *MDM2*, which attributed to p53 stability, was elevated when p53 expression was suppressed. However, overexpression or silence of *DACH1* had no significant effect on *SIX1* protein expression. *DACH1* overexpression elevated expressions of p53, inhibited expressions of *MDM2* and had no marked influence of *SIX1* expression (Fig. 5D-E, $P < 0.05$). The combination of overexpressed *SIX1* and decreased expression of *DACH1* further decreased p53 expression and induced hepatocellular carcinoma.

Effects of *SIX1*/*DACH1* on HCC cell growth in vivo

In order to further observe the effect of *SIX1* and *DACH1* overexpression on tumor growth *in vivo*, stably infected cells were

injected into nude mice. In blank group, HepG2 cells without any treatment were injected into mice; in negative control group, HepG2 cells infected with pc3.1 empty vector were injected into mice; in cDNA-*SIX1* group and in cDNA-*DACH1* group respectively, HepG2 cells infected with cDNA-*SIX1* vector or cDNA-*DACH1* were injected into mice. Fig. 6A showed tumor growth in different groups after resection. Changes in tumor size (Fig. 6B&6D) and tumor weight (Fig. 6C) validated that *SIX1* overexpression promoted tumor growth and *DACH1* overexpression alleviate tumor growth. In cDNA-*SIX1* group, tumors had the faster growth rate and larger tumor size as compared with NC group. In cDNA-*DACH1* group, tumors displayed the lower growth rate and smaller tumor size as compared with NC group (Fig. 6B&6D, $P < 0.05$). Tumor weight

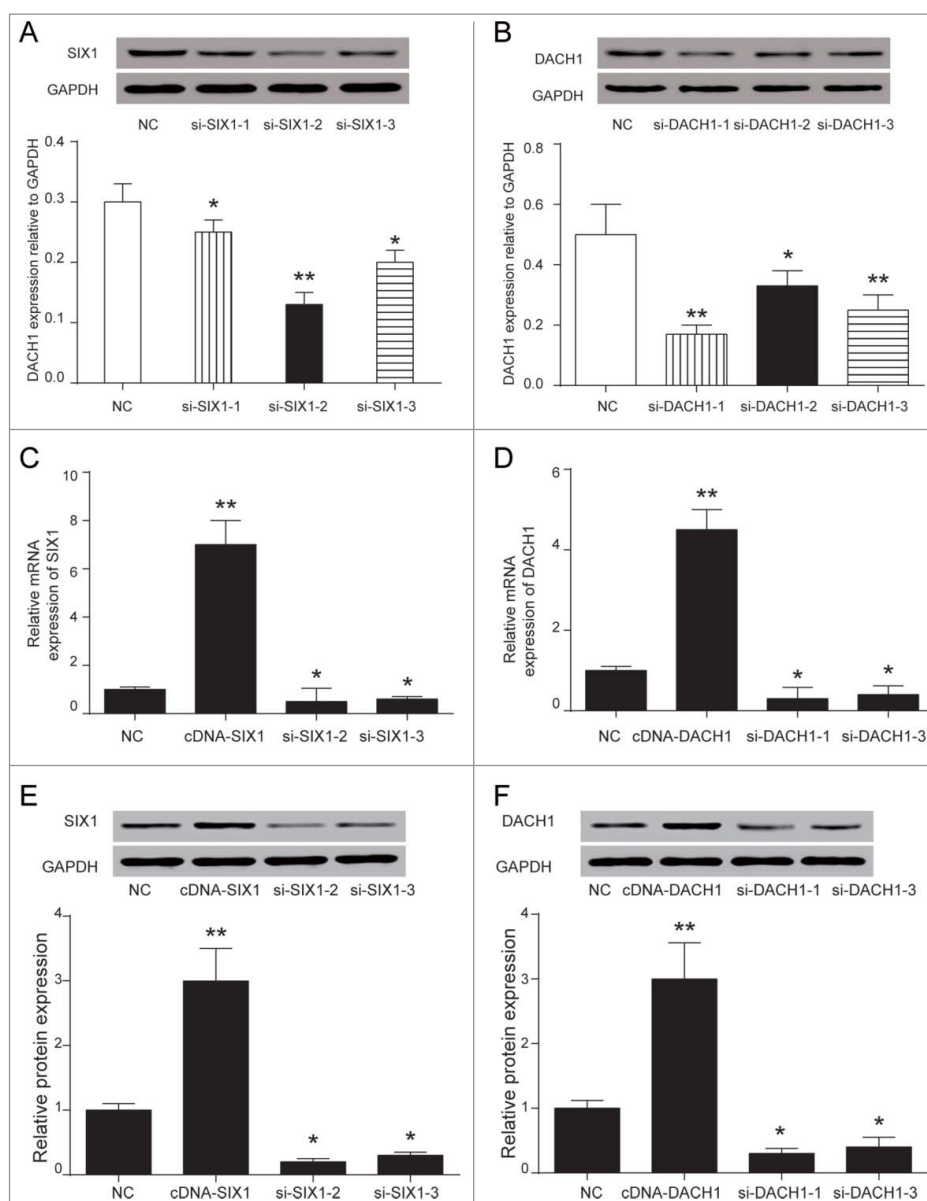


Figure 2. SiRNAs could significantly inhibit *SIX1* and *DACH1* expressions. (A-B) WB results showed that si-SIX1-2 had the best inhibition efficiency of *SIX1* expression and si-DACH1-1 had the best inhibition efficiency. (C&E) QPCR and WB verified high expression of *SIX1* in cDNA-*SIX1* group and low expression of *SIX1* in si-SIX1-2 group and si-SIX1-3 group. (D&F) QPCR and WB verified high expression of *DACH1* in cDNA-*DACH1* group and low expression of *DACH1* in si-DACH1-1 and si-DACH1-3 group.

showed significant increase at day 28 in cDNA-*SIX1* group and great decrease in cDNA-*DACH1* group (Fig. 6C, $P < 0.05$). Protein expressions were tested in resected tumors to validate that tumor growth changes were caused by *SIX1*/*DACH1*/p53 expression fluctuations. *DACH1* and p53 were negatively correlated with *SIX1*; *DACH1* exerted no effect on the expression of *SIX1* but positively regulated the expression of p53 (Fig. 6E, $P < 0.05$). Therefore, *SIX1* could inhibit the expression of *DACH1* which could positively regulated p53 protein and inhibit tumor growth primarily.

Discussion

In the present study, we screened out *SIX1*, highly expressed in HCC tissues and cells, and *DACH1* with low expression in HCC tissues and cells. *SIX1* promoted cell proliferation and inhibited cell apoptosis while *DACH1* impeded cell

proliferation, promoted cell apoptosis and retarded cell cycle. Additionally, we found that *SIX1* overexpression could inhibit p53 by suppressing *DACH1*, which also promoted tumor growth. Therefore *SIX1*/*DACH1*/p53 axis may be the underlying modulation mechanism of HCC progression.

As for *SIX1*, it is a member of SIX families (SIX1-6) of homeobox genes and is an important regulator in cancer. Studies have found that *SIX1* stimulated tumor progression. For instance, Zeng et al. found that the overexpression of *SIX1* positively correlated with the growth of prostate cancer.¹⁴ Lerbs demonstrated the inhibition of *SIX1* suppressed pancreatic cancer.¹⁵ What's more, *SIX1* contributes to the progression of glioblastoma cell and tumor growth.¹⁶ In this study, *SIX1* overexpression could promote cell proliferation and inhibit cell apoptosis, which is consistent with the findings of previous studies.

DACH1 belongs to Retinal Determination Gene Network (RDGN), which mainly includes Dach, Eya and Six family

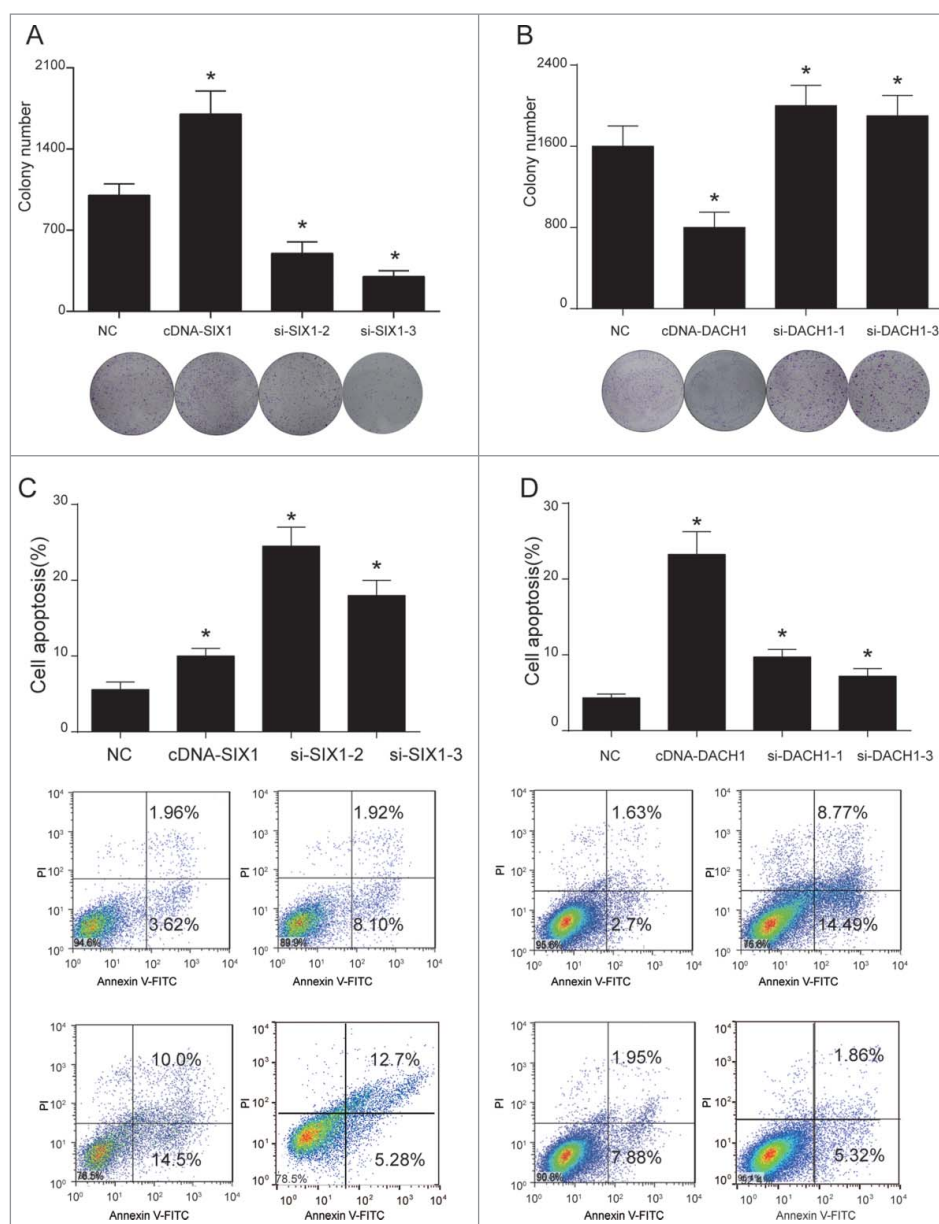


Figure 3. SIX1 promoted proliferation and inhibited apoptosis while DACH1 had an opposite effect. (A-B) SIX1 promoted proliferation while DACH1 inhibited proliferation. The overexpression of *SIX1* and suppression of *DACH1* promoted cell proliferation by colony formation assay. On the contrary, the suppression of *SIX1* and overexpression of *DACH1* inhibited cell proliferation. $P < 0.05$ indicated significant difference compared with NC group. (C-D) *SIX1* inhibited cell apoptosis and *DACH1* promoted cell apoptosis. The overexpression of *SIX1* and the inhibition of *DACH1* suppressed cell apoptosis. Oppositely, the inhibition of *SIX1* and overexpression of *DACH1* promoted cell apoptosis.

members. Studies have shown that *DACH1* actively participated in tumor inhibition. For example, Chu et al. demonstrated that *DACH1* inhibited renal cancer cell propagation and tumor growth.¹⁷ Han et al. reported that *DACH1* could also restrain lung adenocarcinoma aggressiveness by blocking *CXCL5* signaling.¹⁸ Wu et al. found that the silencing of *DACH1* was also vital for esophageal cancer growth.¹⁹ Here, same as previous discoveries, we found the tumor inhibition role of *DACH1* in HCC.

It is known that p53 is highly connected with the pathway of apoptosis and contributes to anticancer progresses.¹¹ CD147 promoted cell proliferation in HCC cells by inhibiting the p53-dependent signaling pathway.²⁰ MiR-221 sustained cell-cycle progression and apoptotic response to doxorubicin in hepatocellular carcinoma-derived cell lines by modulating p53/mdm2

feedback loop.²¹ Therefore, p53 acts as an important modulator in tumor progression, which was found to be regulated by *SIX1/DACH1* in this study.

However, the limitation of this study should be taken into consideration. For example, the cell lines chosen for colony-formation assays are not so representative; although we have examined the correlation between *SIX1*, *DACH1* and p53 and their effects on HCC, the specific interaction mechanism, especially the correlation between *SIX1* and p53 has not been elucidated and needs further study.

In conclusion, we have found that *SIX1* was high expressed and *DACH1* was low expressed in hepatocellular carcinoma tissues and cells; *SIX1* overexpression and *DACH1* suppression accelerated HCC cells progression. Moreover, we have excavated the mechanism of *SIX1*, *DACH1* and p53 regulation:

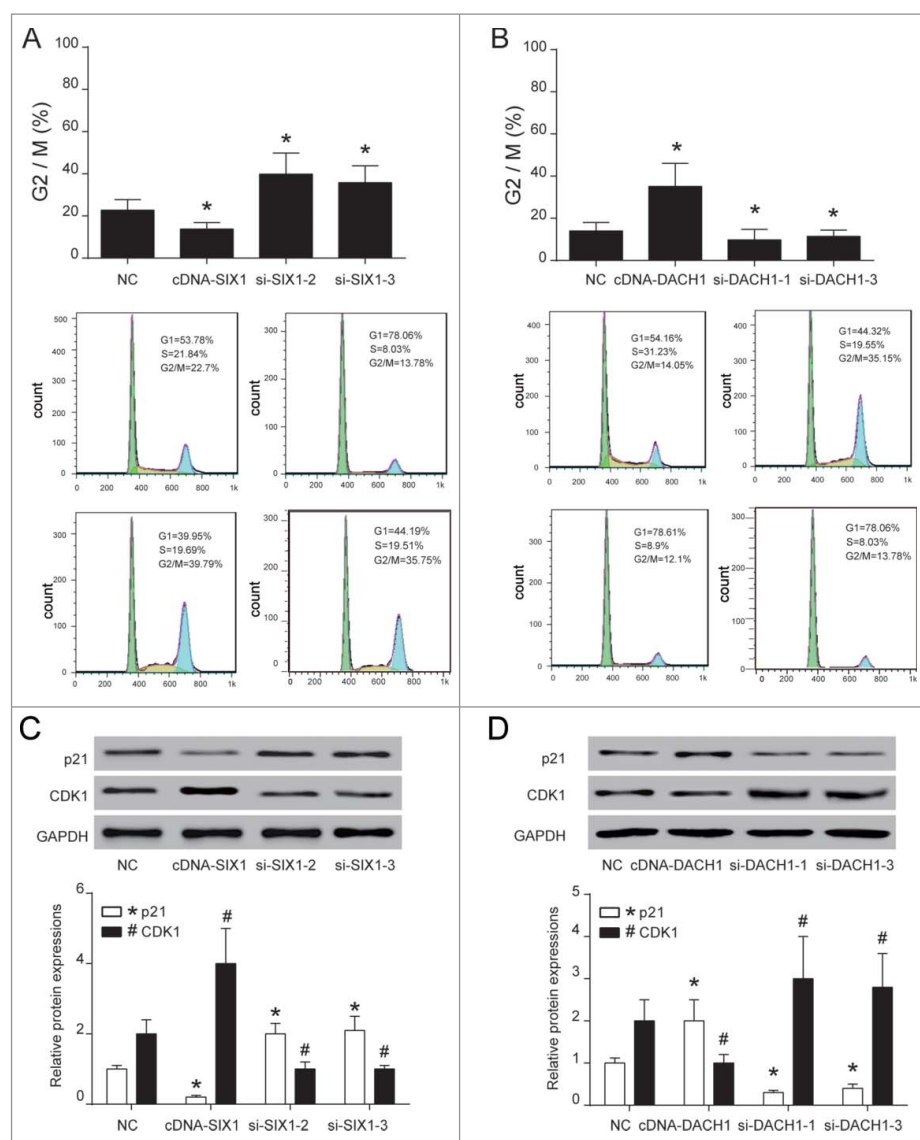


Figure 4. *SIX1* promoted cell cycle while *DACH1* retarded cell cycle. (A-B) *SIX1* suppression and *DACH1* overexpression retarded cell cycle at G2/M phase. However, *SIX1* overexpression and *DACH1* suppression greatly reduced cells that retarded at G2/M phase. (C-D) p21 expression was elevated and CDK1 expression was inhibited when cell cycle was retarded. p21 expression was suppressed and CDK1 expression was improved when *SIX1* was overexpressed and *DACH1* was suppressed. Reversely, p21 expression was elevated and CDK1 expression was suppressed when *SIX1* was inhibited and *DACH1* was overexpressed. $P < 0.05$ indicated significant difference compared with NC group.

SIX1 could bind to *DACH1*, which further decreased p53 expression in hepatocellular carcinoma, and induced tumor progression. Our findings provided a new sight for mechanisms of *SIX1/DACH1/p53* regulation and may have potential clinical significance in hepatocellular carcinoma.

Materials and methods

Patient samples

Fifty hepatocellular carcinoma tissue and para-cancerous tissue specimens were collected at Affiliated Tongji Hospital, Tongji Medical College, Huazhong University of Science and Technology. Patient tissue samples were surgically resected without radiotherapy and chemotherapy. The tissues were immediately frozen in liquid nitrogen and stored at -80°C until total RNAs or proteins extraction. The study was approved by the Ethics Committees at Affiliated Tongji Hospital, Tongji Medical

College, Huazhong University of Science and Technology, and informed consent on revised version of Declaration of Helsinki was obtained from each patient.

Cell culture and transfection

Non-metastatic human HCC cell lines HepG2, Huh-7, SK-HEP-1 and human normal hepatocytes HL-7702 [L-02], HEK293T cells were purchased from BNCC (Beijing, China). HL-7702, HepG2 and Huh-7 cells were cultured in 90% FBS and 10% DMSO. SK-HEP-1 Cells were cultured in 50% RPMI-1640, 40% FBS and 10% DMSO. All reagents were purchased from BeNa Culture Collection (Beijing, China). For a transient transfection, siRNAs were designed and commercially obtained from to target *SIX1* and *DACH1* as shown in Table 1. The pcDNA3.1 plasmid was double-digested by HpaI and XhoI enzymes followed by inserting human *SIX1* or *DACH1* cDNA into nuclear acids of the pc3.1 vector to develop the cDNA-

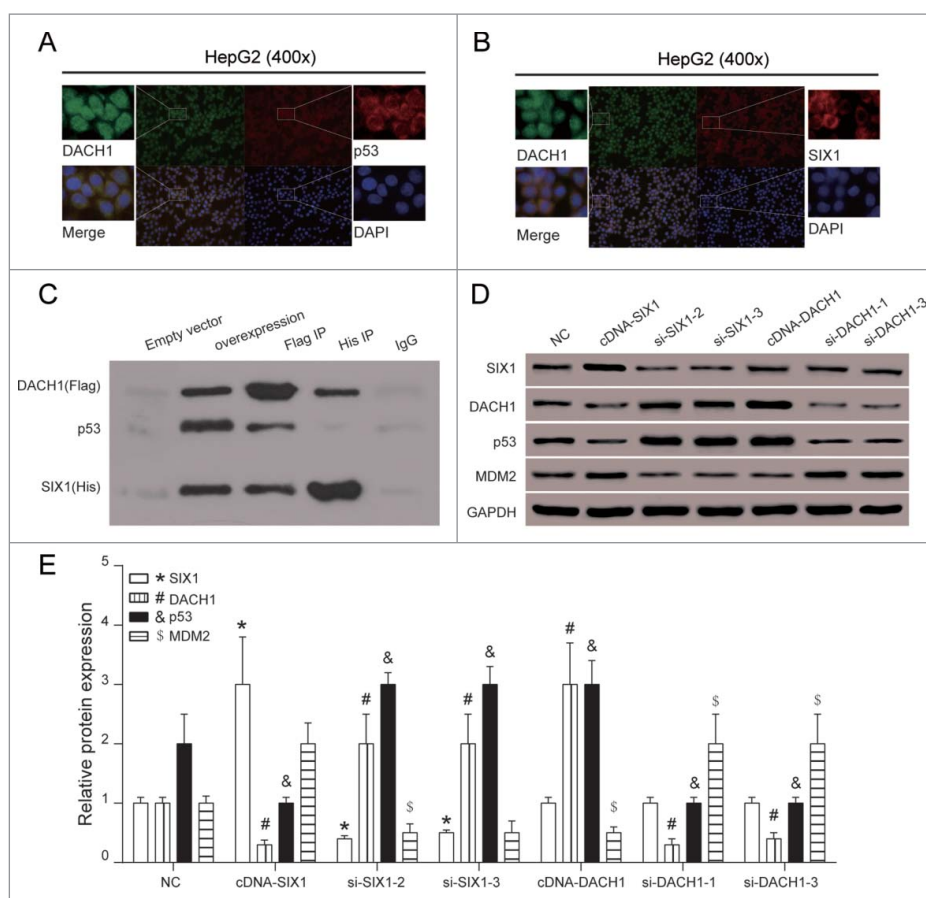


Figure 5. *SIX1/DACH1* regulated p53 expression. (A-B) Immunofluorescence co-localization observed that the relative position of p53 protein and *SIX1* protein overlap significantly, indicating possible combination. (C) *SIX1* co-precipitated with *DACH1* and *DACH1* co-precipitated with *SIX1* and p53. In overexpression group, *DACH1*, p53 and *SIX1* were detected. In Flag IP group, *DACH1* directly interacted with *SIX1* and p53. In His IP group, *SIX1* directly interacted with p53 only. (D-E) *SIX1* suppressed *DACH1* and p53 expression but *DACH1* could only influence p53 expression. *SIX1* overexpression inhibited *DACH1* and p53 protein expression and promoted MDM2 expression. *SIX1* suppression promoted *DACH1* and p53 protein expression and inhibited MDM2 expression. *DACH1* overexpression promoted p53 expression and inhibited MDM2 expression. *DACH1* suppression inhibited p53 expression and promoted MDM2 expression. * $P < 0.05$ indicated significant difference compared with NC group. #, &, \$ $P < 0.05$ indicated statistical significance compared with NC group.

SIX1 vector and cDNA-*DACH1* vector. Cells were seeded in six-well plates at 2×10^4 cells/well and cultured to 80% confluence. Transfection was performed by using Lipofectamine 2000 (Invitrogen, Carlsbad, CA, USA) according to the manufacturer's instruction.

Microarray analysis

RNA for gene expression analysis was obtained from fifty hepatocellular carcinoma tissue and para-cancerous tissue specimens. GeneChip Human Genome U133 Plus 2.0 Array (Affymetrix) were used for these studies and detailed information was indicated in Table 2. Assays of triplicate samples were performed at the core facility at the Affiliated Tongji Hospital, Tongji Medical College, Huazhong University of Science and Technology.

RT-qPCR

Total RNA was isolated using TRIzol™ Plus RNA Purification Kit (Invitrogen, USA). First-strand cDNA for real-time quantitative PCR analysis was synthesized from five micrograms of total RNA using SuperScript™ III Reverse Transcriptase kit

(Invitrogen). Reverse transcription of mRNA was carried out using TaqMan high-capacity cDNA kit (Thermo Fisher Scientific, USA) with GAPDH as internal control. Applied Biosystems StepOne real-time PCR was used for testing. Cycling parameters were as follows: initial denaturation for 3 min at 95°C, followed by 45 cycles of 5 s at 95°C and 30 s at 60°C. Calculations of relative gene expression in treatment samples versus controls were performed using the $2^{-\Delta\Delta C_t}$ method. Primers are listed in Table 3.

Western blot

Frozen tissue or HCC cells were lysed using RIPA buffer (Cell Signaling, USA, #9806). The collected protein lysates were quantitatively prepared to a consistent concentration using a BCA kit (Beyotime Biotechnology, Shanghai, China, Lot # P0012S). Protein extracts were separated by 12% SDS-PAGE and transferred to PVDF membranes (Millipore, Billerica, MA, USA). After being blocked with 5% nonfat milk at room temperature for 1 h, properly diluted primary antibodies (Abcam, USA, #ab211359, #ab176718, #ab9485) were hybridised with the membranes at 4°C overnight. The membrane was washed for three times with TBST for 10 min and incubated with

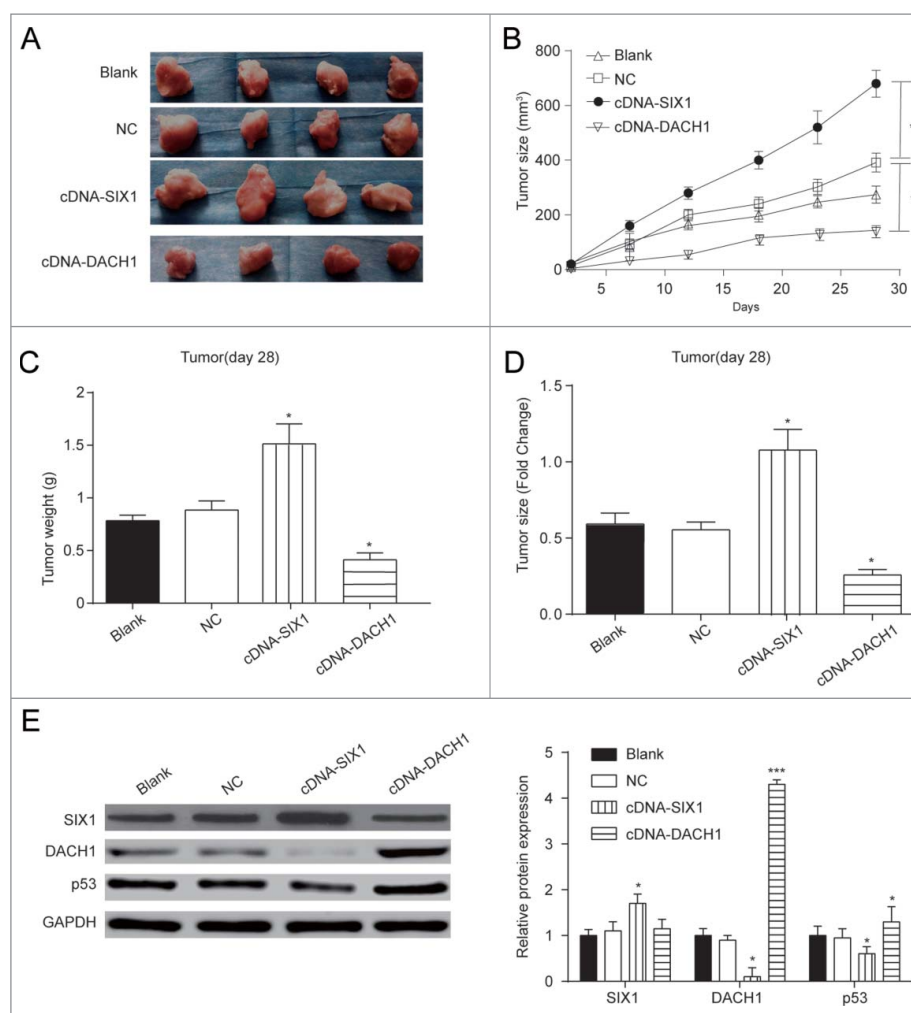


Figure 6. Effects of SIX1/DACH1 on tumor growth *in vivo*. (A&B&D) SIX1 promoted tumor growth and DACH1 inhibited tumor growth. Tumor size in cDNA-SIX1 group was the largest, and in cDNA-DACH1 group was the smallest. (C) Tumor in cDNA-SIX1 group was the heaviest, and in cDNA-DACH1 group was the lightest on day 28. (E) SIX1 was highly expressed, DACH1 was lowly expressed and p53 was lowly expressed in large tumors. On the contrary, SIX1 was lowly expressed, DACH1 was highly expressed and p53 was highly expressed in small tumors. * $P < 0.05$ indicated significant difference compared with Blank and NC group.

secondary antibodies (Abcam, #ab97095) at room temperature for over 1 h. Band signals were determined using ECL Plus system (GE Healthcare UK Ltd., Buckinghamshire, UK).

Colony-formation assays

Transfected cells were seeded onto a 6-well plate and incubated in normal condition. After 2 weeks of cultivation, cells were fixed by ice-cold methanol for 30 min and stained by 0.04% crystal violet for 10 min in methanol for 30 min. Colonies (more than 50 cells) were counted directly on the plate. A light microscope was used to observe the number of cell colonies and statistical significance was calculated from three independent experiments.

Cell apoptosis analysis

Quantification of apoptotic cells was performed according to the Annexin-V-fluorescein isothiocyanate (FITC) manufacturer's instructions (KeyGen Biotech, Nanjing, China). Cells were harvested and fixed overnight with 70% ethanol at 4°C, followed by resuspension in 500 μ L of PBS. Then 2 μ L

Annexin-V-FITC and 5 μ L of PI were added. Analyses were performed by a flow cytometer (BD FACScan) with Ex = 488 nm, Em = 530 nm. FITC-positive and PI-negative cells were regarded as apoptotic cells. The sample was incubated for 5 minutes in the dark before analysis by a flow cytometer (BD Biosciences, San Jose, CA).

Immunofluorescent localization

HepG2 cells counting 3×10^4 were plated onto slides for 48 h growth in advance of the experiment. Cells were then washed with phosphate buffered saline (PBS) prior to fixation for 15 min with 4% ice-cold paraformaldehyde (PFA). Following the fixation, cells were permeated using 0.1% (w/v) Triton X-100 (Sigma-Aldrich) in PBS for 3 \times 5 min and blocked by 5% BSA at 37°C for 30 min, incubated with primary antibodies anti-DACH1 (Abcam, #ab176718), anti-SIX1 (Abcam, #ab211359) or anti-p53 (Santa Cruz Biotechnology, USA, #SC-126) at 37°C for 2 h, and stained with Alexa Fluor 488-conjugated or 568-conjugated IgG at 37°C for 1 h. Meanwhile, the nuclei were stained with DAPI, and the images were collected using fluorescence microscopy.

Table 1. siRNA design.

	sense(5'–3')	anti-sense(3'–5')
siRNA-SIX1–1	GCTGCAGCGAAAGTTCATG	CATGAACCTTCGCTGCAGC
siRNA-SIX1–2	GCAGCGAAAGTTCATGAAC	GTTTCATGAACCTTCGCTGC
siRNA-SIX1–3	GCCTCATTGCTTTGAGCA	TGCTCAAAGCAAATGAGGC
siRNA-SIX1-control	GCTGCGAGAACTTCGATG	CATCGAAGTTTCTCGCAGC
siRNA-DACH1–1	GCCTCCTAAGAGGACTCAA	TTGAGTCTCTTAGGAGGC
siRNA-DACH1–2	CCTCCTAAGAGGACTCAA	TTGAGTCTCTTAGGAGG
siRNA-DACH1–3	CTGCTACCAATGCAGCTA	TAGCTGCATTGGTAGCAG
siRNA-DACH1-control	GCCAATCGGAGTCACTCAA	TTGAGTGACTCCGATTGGC

Table 2. SIX1 and DACH1 expressions in hepatocarcinoma.

	logFC	AveExpr	P.Value
SIX1	12.54685664	–5.12529851	3.92E-14
DACH1	–2.885306989	4.59281158	7.63E-25

Immunoprecipitation

Amplified DACH1 cDNA was inserted into pCMV-flag plasmids (Riobio, Guangzhou, China) and SIX1 cDNA was subcloned into pCMV-his plasmid (Riobio). HEK 293T cells were transfected with pFLAG-DACH1, pCMV-his-SIX1 and pCMV-p53 (Riobio) one by one to overexpress flag-DACH1, his-SIX1 and p53. Selection with G418 was performed after each transfection. Transfected 293T cells were harvested in Tris-NaCl-EDTA (TNE) buffer (10 mM Tris-HCl, pH 7.8, 0.15 M NaCl, 1 mM ethylenediaminetetraacetic acid and 1% Nonidet P-40) supplemented with a protease inhibitor cocktail (Roche Diagnostics). Cell lysates were pre-absorbed with mouse IgG-agarose and subsequently incubated with an anti-His antibody (Invitrogen) for 2 h at 4°C and then for 1 h with anti-Flag affinity gel (Sigma-Aldrich). The beads were then added and the incubation was performed at 4°C for 3 hours. Afterwards, each tube was centrifuged at 5,000 rpm for 5 minutes at 4°C. The supernatant was obtained and stored in microcentrifuge tubes at –80°C. The beads were then washed five times with TNE buffer, and the immunoprecipitated proteins were examined by western blot analysis. All experiments were performed at least twice.

Nude mice study

Animal handling and experimental procedures were approved by the Affiliated Tongji Hospital, Tongji Medical College, Huazhong University of Science and Technology. We inoculated transfected cells subcutaneously into nude mice aging

Table 3. Oligonucleotide primer sequences.

oligonucleotide	primer sequences
qPCR-DACH1	Forward 5'-GGAATGGATTGTGGCTGAAC-3' Reverse 5'-GGTATTGGACTGGTACATCAAG-3'
qPCR-SIX1	Forward 5'-AAGGAGAAGTCGAGGGGTGT-3' Reverse 5'-TGCTTGTTGGAGGAGGAGTT-3'
qPCR-GAPDH	Forward 5'-AGTAGAGGCAGGGATGATG-3' Reverse 5'-TGGTATCGTGGAAAGGACTC-3'
DACH1-cDNA	Forward 5'-GGATCCATGTCTGATGCTGCCGTCG-3' Reverse 5'-TCTAGATTAGGACCCCAAGTCC-3'
SIX1-cDNA	Forward 5'-GGATCCACATGGCAGTCCGGCGGC-3' Reverse 5'-TCTAGATCAGTACATGACAGTAG-3'

4–6 weeks purchased from the National Cancer Institute, NIH. The tumor growth was measured every 7 days for 4 times by using a digital caliper since day 7 and graphs were drawn. Tumor weight was measured when mice were sacrificed on day 28 after cell implantation. We measured tumor diameters every other day, and calculated tumor volume (mm³) as follows: volume = (shortest diameter)² × (longest diameter) × 0.5.

Statistics analysis

All statistical analysis was performed using Graphpad statistical software, and the data was expressed as mean standard deviation (mean±SD). The Student's t-test and one-way ANOVA were applied to evaluate the differences in groups as appropriate and the significance level was set at 0.05.

Ethical approval

The study was approved by the Ethics Committees at Affiliated Tongji Hospital, Tongji Medical College, Huazhong University of Science and Technology, and informed consent on revised version of Declaration of Helsinki was obtained from each patient.

Disclosure of potential conflicts of interest

No potential conflicts of interest were disclosed.

Acknowledgments

None.

Funding

This work was supported by the National Natural Science Foundation of China (NSFC) (No. 81700571 and No. 81472705).

Author contribution

Research conception and design: Deng Ning
Data analysis and interpretation: Jin Chen and Xue Li
Statistical analysis: Xue Li and Qi Cheng
Drafting of the manuscript: Qi Cheng
Critical revision of the manuscript: Xiaoping Chen and Li Jiang
Receiving grant: Li Jiang
Approval of final manuscript: all authors.

References

- Zhu H, Wu K, Yan W, Hu L, Yuan J, Dong Y, Li Y, Jing K, Yang Y, Guo M. Epigenetic silencing of DACH1 induces loss of transforming growth factor-beta1 antiproliferative response in human hepatocellular carcinoma. *Hepatology*. 2013;58(6):2012–22. doi.org/10.1002/hep.26587 PMID:23787902.
- Suen AA, Jefferson WN, Wood CE, Padilla-Banks E, Bae-Jump VL, Williams CJ. SIX1 oncoprotein as a biomarker in a model of hormonal carcinogenesis and in human endometrial cancer. *Mol Cancer Res*. 2016;14(9):849–58. doi.org/10.1158/1541-7786.MCR-16-0084 PMID:27259717.
- Xu H, Zhang Y, Pena MM, Pirisi L, Creek KE. Six1 promotes colorectal cancer growth and metastasis by stimulating angiogenesis and recruiting tumor-associated macrophages. *Carcinogenesis*. 2017;38(3):281–92. doi.org/10.1093/carcin/bgw121 PMID:28199476.

4. Chao L, Liu J, Zhao D. Increased Six1 expression is associated with poor prognosis in patients with osteosarcoma. *Oncol Lett.* 2017;13(5):2891–96. doi.org/10.3892/ol.2017.5803 PMID:28521394.
5. Wu K, Chen K, Wang C, Jiao X, Wang L, Zhou J, Wang J, Li Z, Addya S, Sorensen PH, et al. Cell fate factor DACH1 represses YB-1-mediated oncogenic transcription and translation. *Cancer Res.* 2014;74(3):829–39. doi.org/10.1158/0008-5472.CAN-13-2466 PMID:24335958.
6. Chen K, Wu K, Cai S, Zhang W, Zhou J, Wang J, Ertel A, Li Z, Rui H, Quong A, et al. Dachshund binds p53 to block the growth of lung adenocarcinoma cells. *Cancer Res.* 2013;73(11):3262–74. doi.org/10.1158/0008-5472.CAN-12-3191 PMID:23492369.
7. Lee JW, Kim HS, Kim S, Hwang J, Kim YH, Lim GY, Sohn WJ, Yoon SR, Kim JY, Park TS, et al. DACH1 regulates cell cycle progression of myeloid cells through the control of cyclin D, Cdk 4/6 and p21Cip1. *Biochem Biophys Res Commun.* 2012;420(1):91–5. doi.org/10.1016/j.bbrc.2012.02.120 PMID:22405764.
8. Martik ML, McClay DR. Deployment of a retinal determination gene network drives directed cell migration in the sea urchin embryo. *Elife.* 2015;4:e08827. doi.org/10.7554/eLife.08827 PMID:26402456.
9. Liu Y, Han N, Zhou S, Zhou R, Yuan X, Xu H, Zhang C, Yin T, Wu K. The DACH/EYA/SIX gene network and its role in tumor initiation and progression. *Int J Cancer.* 2016;138(5):1067–75. doi.org/10.1002/ijc.29560 PMID:26096807.
10. Miller SJ, Lan ZD, Hardiman A, Wu J, Kordich JJ, Patmore DM, Hegde RS, Cripe TP, Cancelas JA, Collins MH, et al. Inhibition of eyes absent Homolog 4 expression induces malignant peripheral nerve sheath tumor necrosis. *Oncogene.* 2010;29(3):368–79. doi.org/10.1038/onc.2009.360 PMID:19901965.
11. Kuo PL, Lin TC, Lin CC. The antiproliferative activity of aloë-emodin is through p53-dependent and p21-dependent apoptotic pathway in human hepatoma cell lines. *Life Sci.* 2002;71(16):1879–92. PMID:12175703
12. Meng X, Franklin DA, Dong J, Zhang Y. MDM2-p53 pathway in hepatocellular carcinoma. *Cancer Res.* 2014;74(24):7161–7. doi.org/10.1158/0008-5472.CAN-14-1446 PMID:25477334.
13. Lahav G, Rosenfeld N, Sigal A, Geva-Zatorsky N, Levine AJ, Elowitz MB, Alon U. Dynamics of the p53-Mdm2 feedback loop in individual cells. *Nat Genet.* 2004;36(2):147–50. doi.org/10.1038/ng1293 PMID:14730303.
14. Zeng J, Shi R, Cai CX, Liu XR, Song YB, Wei M, Ma WL. Increased expression of Six1 correlates with progression and prognosis of prostate cancer. *Cancer Cell Int.* 2015;15:63. doi.org/10.1186/s12935-015-0215-z PMID:26161040.
15. Lerbs T, Bisht S, Scholch S, Pecqueur M, Kristiansen G, Schneider M, Hofmann BT, Welsch T, Reissfelder C, Rahbari NN, et al. Inhibition of Six1 affects tumour invasion and the expression of cancer stem cell markers in pancreatic cancer. *BMC Cancer.* 2017;17(1):249. doi.org/10.1186/s12885-017-3225-5 PMID:28388884.
16. Tian T, Li A, Lu H, Luo R, Zhang M, Li Z. Six1 promotes glioblastoma cell proliferation and invasion by upregulation of connective tissue growth factor. *Am J Cancer Res.* 2015;5(5):1823–30. PMID:26175950
17. Chu Q, Han N, Yuan X, Nie X, Wu H, Chen Y, Guo M, Yu S, Wu K. DACH1 inhibits cyclin D1 expression, cellular proliferation and tumor growth of renal cancer cells. *J Hematol Oncol.* 2014;7:73. doi.org/10.1186/s13045-014-0073-5 PMID:25322986.
18. Han N, Yuan X, Wu H, Xu H, Chu Q, Guo M, Yu S, Chen Y, Wu K. DACH1 inhibits lung adenocarcinoma invasion and tumor growth by repressing CXCL5 signaling. *Oncotarget.* 2015;6(8):5877–88. doi.org/10.18632/oncotarget.3463 PMID:25788272.
19. Wu L, Herman JG, Brock MV, Wu K, Mao G, Yan W, Nie Y, Liang H, Zhan Q, Li W, et al. Silencing DACH1 promotes esophageal cancer growth by inhibiting TGF-beta signaling. *PLoS One.* 2014;9(4):e95509. doi.org/10.1371/journal.pone.0095509 PMID:24743895.
20. Huang Q, Li J, Xing J, Li W, Li H, Ke X, Zhang J, Ren T, Shang Y, Yang H, et al. CD147 promotes reprogramming of glucose metabolism and cell proliferation in HCC cells by inhibiting the p53-dependent signaling pathway. *J Hepatol.* 2014;61(4):859–66. doi.org/10.1016/j.jhep.2014.04.035 PMID:24801417.
21. Ren ZJ, Nong XY, Lv YR, Sun HH, An PP, Wang F, Li X, Liu M, Tang H. Mir-509-5p joins the Mdm2/p53 feedback loop and regulates cancer cell growth. *Cell Death Dis.* 2014;5:e1387. doi.org/10.1038/cddis.2014.327 PMID:25144722.